



ELSEVIER

Contents lists available at ScienceDirect

## Metabolic Engineering

journal homepage: [www.elsevier.com/locate/ymben](http://www.elsevier.com/locate/ymben)

# Genome-scale metabolic network modeling results in minimal interventions that cooperatively force carbon flux towards malonyl-CoA

Peng Xu<sup>a,1</sup>, Sridhar Ranganathan<sup>b,1</sup>, Zachary L. Fowler<sup>c</sup>, Costas D. Maranas<sup>d</sup>, Mattheos A.G. Koffas<sup>a,\*</sup>

<sup>a</sup> Department of Chemical and Biological Engineering, Center for Biotechnology and Interdisciplinary Studies, Rensselaer Polytechnic Institute, Troy, NY 12180, USA

<sup>b</sup> Huck Institutes of Life Sciences, Pennsylvania State University, University Park, PA 16802, USA

<sup>c</sup> Praxair, Inc., BioPharma Division, Burr Ridge, IL 60527, USA

<sup>d</sup> Department of Chemical Engineering, Pennsylvania State University, University Park, PA 16802, USA

## ARTICLE INFO

## Article history:

Received 24 May 2011

Received in revised form

26 June 2011

Accepted 28 June 2011

## Keywords:

*Escherichia coli*

Metabolic network modeling

Malonyl-CoA

OptForce

Synergistic effect

Flavonoids

## ABSTRACT

Malonyl-coenzyme A is an important precursor metabolite for the biosynthesis of polyketides, flavonoids and biofuels. However, malonyl-CoA naturally synthesized in microorganisms is consumed for the production of fatty acids and phospholipids leaving only a small amount available for the production of other metabolic targets in recombinant biosynthesis. Here we present an integrated computational and experimental approach aimed at improving the intracellular availability of malonyl-CoA in *Escherichia coli*. We used a customized version of the recently developed OptForce methodology to predict a minimal set of genetic interventions that guarantee a prespecified yield of malonyl-CoA in *E. coli* strain BL21 Star<sup>TM</sup>. In order to validate the model predictions, we have successfully constructed an *E. coli* recombinant strain that exhibits a 4-fold increase in the levels of intracellular malonyl-CoA compared to the wild type strain. Furthermore, we demonstrate the potential of this *E. coli* strain for the production of plant-specific secondary metabolites naringenin (474 mg/L) with the highest yield ever achieved in a lab-scale fermentation process. Combined effect of the genetic interventions was found to be synergistic based on a developed analysis method that correlates genetic modification to cell phenotype, specifically the identified knockout targets ( $\Delta fumC$  and  $\Delta sucC$ ) and overexpression targets (ACC, PGK, GAPD and PDH) can cooperatively force carbon flux towards malonyl-CoA. The presented strategy can also be readily expanded for the production of other malonyl-CoA-derived compounds like polyketides and biofuels.

© 2011 Elsevier Inc. All rights reserved.

## 1. Introduction

The biosynthesis of plant-specific secondary metabolites such as aromatic polyketides (Askenazi et al., 2003; Zhang et al., 2008), flavanones (Chemler and Koffas, 2008; Winkel-Shirley, 2001) and fatty acids (Cahoon et al., 2007; Schwender, 2008) has recently become the focus of extensive research efforts due to their pharmaceutical potential in chronic diseases such as diabetes, cancer, obesity and Parkinson's disorder. As a result, tremendous effort has been dedicated to the development of cost-efficient processes for the synthesis of these compounds, which are still manufactured by extraction from their native plant sources. The major bottleneck in such extraction processes is their relatively low abundance and the complicated downstream purification processes (Cragg et al., 1997). Though simple starting materials

can be used to chemically synthesize these compounds, such chemical processes involve toxic intermediates and extreme reaction conditions that significantly limit their scalability (Chemler and Koffas, 2008; Harborne and Williams, 1975). Recently, however, industrial microbial hosts (e.g. *Escherichia coli* and yeast) have been engineered with multi-gene heterologous pathways to combinatorially produce these chemical compounds from renewable resources. In general, the biochemical routes that lead to the synthesis of these compounds involve acyl-CoA monomers (e.g. acetyl-CoA, malonyl-CoA and propionyl-CoA) as precursors. For example, polyketides are formed in a multi-step decarboxylative condensation by the enzyme polyketide synthase (PKS), which recruits one molecule of malonyl-CoA in each step (Khosla and Keasling, 2003; Pfeifer and Khosla, 2001). On the other hand, the pathway responsible for the synthesis of flavanones involves the enzymes 4-coumaroyl-CoA ligase (4CL), chalcone synthase (CHS) and chalcone isomerase (CHI) and requires three molecules of malonyl-CoA (Leonard et al., 2008; Yan et al., 2005). Malonyl-CoA also serves as a starting point for the synthesis of microdiesel (Kalscheuer et al., 2006) and a host of

\* Corresponding author. Fax: +1 518 276 3405.

E-mail addresses: [pxu999@gmail.com](mailto:pxu999@gmail.com) (P. Xu),

[costas@enr.psu.edu](mailto:costas@enr.psu.edu) (C.D. Maranas), [koffam@rpi.edu](mailto:koffam@rpi.edu) (M.A.G. Koffas).

<sup>1</sup> These authors contributed equally to this article.

various other value-added chemical compounds such as polyunsaturated omega-3 fatty acids (Qi et al., 2004). Therefore, the transfer of malonyl-CoA-dependent metabolic pathways into heterologous hosts for various applications depends on resourceful utilization of malonyl-CoA that is derived from primary metabolism.

In both *E. coli* and yeast the intracellular availability of malonyl-CoA is limited (Takamura and Nomura, 1988) due to its direct association with cell growth and synthesis of phospholipids and fatty acids (Magnuson et al., 1993). With the introduction of new genes in the biosynthetic cascade, it is essential to engineer the bacteria so that a metabolic balance can be achieved between the requirement of malonyl-CoA for cell growth and product synthesis. Hence, efficiently harnessing malonyl-CoA in *E. coli* continues to be one of the largest obstacles for producing natural products such as polyketides and flavanones. Metabolic engineering efforts aimed at improving intracellular malonyl-CoA based on metabolic network inspection have resulted in tuning pathways that are closer in proximity to malonyl-CoA synthesis (Lim et al., 2011). For example, overexpression of acetyl-CoA carboxylase (Leonard et al., 2007; Wattanachaisaereekul et al., 2008) that leads to the formation of malonyl-CoA and deleting enzymes involved in its depletion, such as acetate kinase and alcohol dehydrogenase (Zha et al., 2009), have been reported. While genetic manipulations implemented in these studies have significantly improved the synthesis of malonyl-CoA, numerous metabolic engineering possibilities are yet to be explored.

Computational strain design procedures in the past have predicted interventions away from target pathways that propagate carbon flux through the stoichiometry to further boost yield. In this regard, optimization procedures such as OptKnock (Burgard et al., 2003; Pharkya et al., 2003), OptReg (Pharkya and Maranas, 2006), OptORF (Kim and Reed, 2010), RobustKnock (Tepper and Shlomi, 2009) and CiED (Fowler et al., 2009) have enabled efficient use of flux balance analysis (FBA) as a tool to predict genetic interventions for strain redesign. The ever-increasing size and complexity of genome-scale metabolic models for host microorganisms such as *E. coli* (Feist et al., 2007) and yeast (Dobson et al., 2010; Zomorodi and Maranas, 2010) complicate the task of identifying interventions and motivate the use of algorithms that can address both the complexity and the problem of combinatorial explosion that arises when numerous interventions are attempted. In general, most existing approaches rely on surrogate biological fitness functions (e.g. maximization of biomass or minimization of metabolic adjustments (Segre et al., 2002)) to predict metabolic flux rearrangement following a genetic modification. Despite the presence of a large and fast growing collection of metabolic flux data (Fischer et al., 2004; Sauer, 2006; Schaub et al., 2008) that largely pinpoint the physiological state of the wild-type strain, this information is not utilized at its fullest for the successful re-engineering of the production host. Recently, the OptForce procedure (Ranganathan and Maranas, 2010; Ranganathan et al., 2010) was introduced to directly make use of flux measurements available for the wild-type strain. The procedure is designed to identify the changes in reaction fluxes that must take place in the metabolic network by contrasting the maximum range of flux variability for the wild-type strain against the ones consistent with a prespecified overproduction target. In this study, we demonstrate the utility of OptForce in predicting genetic interventions resulting in significantly improved yields that are far away from the target pathways. OptForce procedure identifies the complete set of minimal genetic intervention strategies using a Boolean description consistent with an overproduction target. Here, we first characterize the wild-type strain of *E. coli*, BL21 Star™ based on available flux measurements and then identify computationally the interventions that cooperatively force carbon

flux towards malonyl-CoA while at the same time preventing the drain towards byproducts. We combinatorially analyzed the impact of gene knockouts and overexpression strategies and demonstrate the sequential aggregation of beneficial interventions. The combined use of computations and experiments to increase the availability of malonyl-CoA is demonstrated for the synthesis of the flavanone molecule naringenin in *E. coli*.

## 2. Materials and methods

### 2.1. Computational procedure

The essence of OptForce procedure is to compare and contrast the maximal range of flux variability for a wild-type strain (or a base strain) against the ones consistent with a prespecified overproduction objective. As outlined in our earlier efforts (Ranganathan and Maranas, 2010; Ranganathan et al., 2010), the flux ranges for the wild-type strain can be elucidated by iteratively maximizing and minimizing each flux in the network (Burgard and Maranas, 2001; Mahadevan and Schilling, 2003) subject to constraints pertaining to stoichiometry, uptakes and environmental conditions (i.e. regulation) and MFA data. The flux measurements used in this procedure can be either exact values or ranges. By superimposing the flux ranges one-at-a-time, we identify the fluxes that must depart from the original ranges in the face of overproduction (MUST sets). We extend this classification procedure by considering sums and differences of two, three or more fluxes and arrive at a collective set of flux changes that must happen in the network for overproduction. The MUST sets represent the set of all changes that must happen in the network. We subsequently extract the minimal subset(s) of these reactions that suffice in guaranteeing the required bioengineering objective (i.e., FORCE sets).

We make use of a max–min bi-level optimization problem (Fig. 1) to identify the minimal set of engineering interventions that forces the yield of the product to the target value. As depicted in Fig. 1, the OptForce procedure identifies metabolic interventions that guarantee the imposed yield even when the network fights against these interventions. Modeled as a worst-case optimization problem, we iteratively solve this problem by increasing the number of direct manipulations ( $k$ ) in each step until the target yield is achieved. OptForce first identifies the interventions that have the largest contribution towards meeting the overproduction target thus providing a way to prioritize the implementation of genetic interventions. We have found that when  $k$  is increased, genetic interventions found before are largely conserved. In addition, at the optimal yield, the use of integer cuts allows for the identification of alternate optimal solutions that can serve as alternate genetic intervention choices.

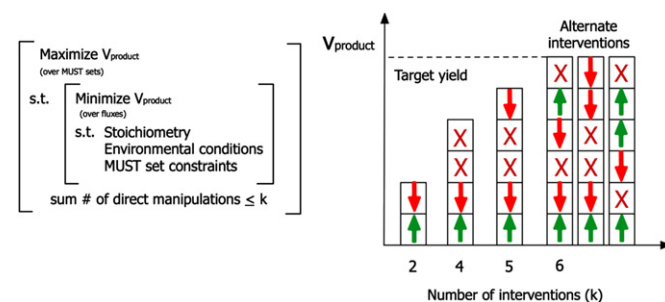


**Fig. 1.** An outline of the OptForce procedure to identify the minimal set of genetic interventions that guarantee the imposed yield: The left panel shows the bi-level optimization algorithm and the right panel outlines the plot between the yield of the product and the number of direct manipulations identified by OptForce.

In this paper, we have deployed OptForce to identify the minimal set of genetic manipulations to improve the malonyl-CoA availability for flavanone synthesis. We have used wild-type flux measurements (Noronha et al., 2000; van de Walle and Shiloach, 1998) for *E. coli* strain BL21 Star<sup>TM</sup>. The latest genome-scale metabolic model for *E. coli* (Feist et al., 2007) was used to perform computations. The reactions in the flavanone synthesis pathways added to the model are shown in Table S1 (Supplemental Table 1) in the supplemental files. All other metabolite and reaction abbreviations used in this paper are consistent with the iAF1260 model.

## 2.2. Strains and media

Strains and plasmids used in this work are listed in Table S2 (Supplemental Table 2) in the supplemental files. All recombinant plasmid construction was performed using *E. coli* XL1-Blue (Stratagene) as a host strain following standard cloning protocols and BL21 Star<sup>TM</sup> (DE3) (Invitrogen) was used for flavanone production. Plasmids pKD4, pKD46 and pCP20 for gene knockout construction were obtained from the *E. coli* Genetic Resource Center, Yale University. The duet vectors pCoLA-Duet and pCDF-Duet (Novagen) were used for cloning and subcloning. Restriction enzymes and T4 DNA ligase were purchased from New England Labs. Genomic DNA was prepared using PureLink genomic DNA purification kit (Invitrogen), and colony PCR was performed using GoTaq HotStart DNA polymerase (Promega); all other PCRs were performed using Phusion High Fidelity Master Mix (Finnzymes). Plasmid DNA preparation and fragment DNA recovery were conducted using the Zippy miniprep kit and Zymoclean gel recovery kit (Zymo Research), respectively. Luria-Bertani (LB) broth (Sigma) and M9 minimal salts (Difco) were routinely used for culture growth and flavanone production. Recombinant cultures were grown in media containing the appropriate antibiotics: ampicillin (70 µg/ml), streptomycin (40 µg/ml), kanamycin (40 µg/ml) and chloramphenicol (20 µg/ml). Culture glucose levels were measured using a Wako LabAssay<sup>TM</sup> Glucose kit (B-Bridge) purchased from Japan. All chemicals were purchased from Sigma unless otherwise specified.

## 2.3. Cloning and pathway construction

All PCR primers used for gene overexpression and knockout are listed in Table S3 (Supplemental Table 3) in the supplemental files. *E. coli* K-12 (MG1655) genomic DNA was used as a template for amplification of *pgk*, *gapA*, *aceE*, *aceF* and *lpdA* genes using the forward and reverse primers specified in Table S3 (Supplemental Table S3). Subsequently, the *pgk* and *gapA* PCR products were double digested, gel purified and cloned into the BamHI/SacI and BglII/XhoI restriction sites of pCoLA-Duet vector, respectively. The *pgk* fragment was then subcloned into the BamHI/SacI sites of pCoLA-*gapA* or pCDF-4CL2, to form pCoLA-*pgk-gapA* or pCDF-*pgk-4CL2* constructs. For overexpression of pyruvate dehydrogenase multienzyme complex, three rounds of cloning were performed. First, the *lpdA* and *aceF* gene were inserted into the BamHI/EcoRI and BglII/XhoI restriction sites of pCoLA-Duet vector, forming plasmids pCoLA-*lpdA* and pCoLA-*aceF*, respectively. Then the T7-*aceF* fragment was amplified and cloned into the Sall/NotI restriction site of pCoLA-*lpdA* to form pCoLA-*lpdA-T7aceF*, using pCoLA-*aceF* as template. Finally, *aceE* fragment was cloned into the MfeI/XhoI restriction sites of pCoLA-*lpdA-T7aceF* to form recombinant plasmid pCoLA-PDH; each of the three subunits (*lpdA*, *aceE* and *aceF*) was under the control of a separate T7 promoter. All clones were screened by restriction digestion analysis and subsequently verified by gene sequencing.

Gene deletions were performed using the red recombinase based chromosomal gene inactivation protocol developed by Datsenko and Wanner (2000). Deletion primers (Table S3) with 40 nt homologous regions were used to create the FRT-flanked kanamycin resistance cassette from pKD4, which was then transformed into the red-recombinase expressing BL21 Star<sup>TM</sup> (DE3) strain by electroporation. Positive knockout strains were screened by colony PCR and verified by gDNA PCR using the genomic DNA as template. Finally, the resistance marker was eliminated by expressing the flippase recombination enzyme from pCP20.

## 2.4. Flavanone fermentation

Flavanone production was performed based on a two-step fermentation protocol. Strains were first cultivated in 40 ml LB broth at 37 °C with orbital shaking. Induction of heterologous pathway expression was performed during the mid-exponential phase of cultivation (approximately OD 0.6–0.8) by addition of 1 mM IPTG and the cultures were allowed to grow at 30 °C for an additional 6–8 h. After induction, the bacterial pellet was harvested by centrifugation and suspended with 16 ml M9 modified medium (1 × M9 salts, 8 g/L glucose, 1 mM MgSO<sub>4</sub>, 0.1 mM CaCl<sub>2</sub>, 6 µM biotin, 10 nM thiamine, 2.6 mM *p*-coumaric acid, 1 mM IPTG). Fermentation was performed in 250 ml batch flasks with orbital shaking at 300 rpm and 30 °C. 4 g/L glucose (0.4%) was supplemented once the glucose was completely exhausted (approximately at 12 and 20 h of cultivation). Flavanones were extracted with 50% ethanol after 24 h of fermentation, then the *E. coli* pellet was removed by ultracentrifugation and the supernatant was analyzed for flavanone quantification. Fermentation kinetics was investigated for every 2 or 3 h by measuring biomass concentration, glucose and *p*-coumaric acid consumption and flavanone production throughout the 40-h fermentation process. Cell growth rate, glucose consumption rate and flavanone production rate were obtained by analyzing the steady state fermentation kinetic curves (usually achieved for the first 10 h fermentation) using linear progression, with a correlation coefficient more than 0.95 used as the selection criteria.

## 2.5. Analytical procedures

Flavanones were analyzed by the Agilent 1100 HPLC system equipped with a ZORBAX SB-C18 column (5 µm, 4.6 × 150 mm) kept at 25 °C and a diode array detector (DAD). The mobile phase contains 35% acetonitrile (with 0.1% formic acid) and 65% water (with 0.1% formic acid). The retention time for *p*-coumaric acid and naringenin were around 2.6 and 6.9 min, respectively. Extraction and quantification of coenzyme A compounds were performed according to the procedures as previously described (Fowler et al., 2009).

## 3. Results

### 3.1. Genetic interventions predicted by OptForce procedure

In this section, we describe all genetic interventions identified by OptForce for improving the intracellular malonyl-CoA levels. Calculations were based on wild-type flux measurements (Noronha et al., 2000; van de Walle and Shiloach, 1998) for *E. coli* strain BL21 Star<sup>TM</sup>. A fixed glucose uptake flux at 100 µmol/gDW/h and a yield of 40 µmol/gDW/h for naringenin while allowing for 50% yield on biomass were imposed as constraints and targets, respectively. Fig. 2 illustrates the results for the FORCE set of genetic interventions.

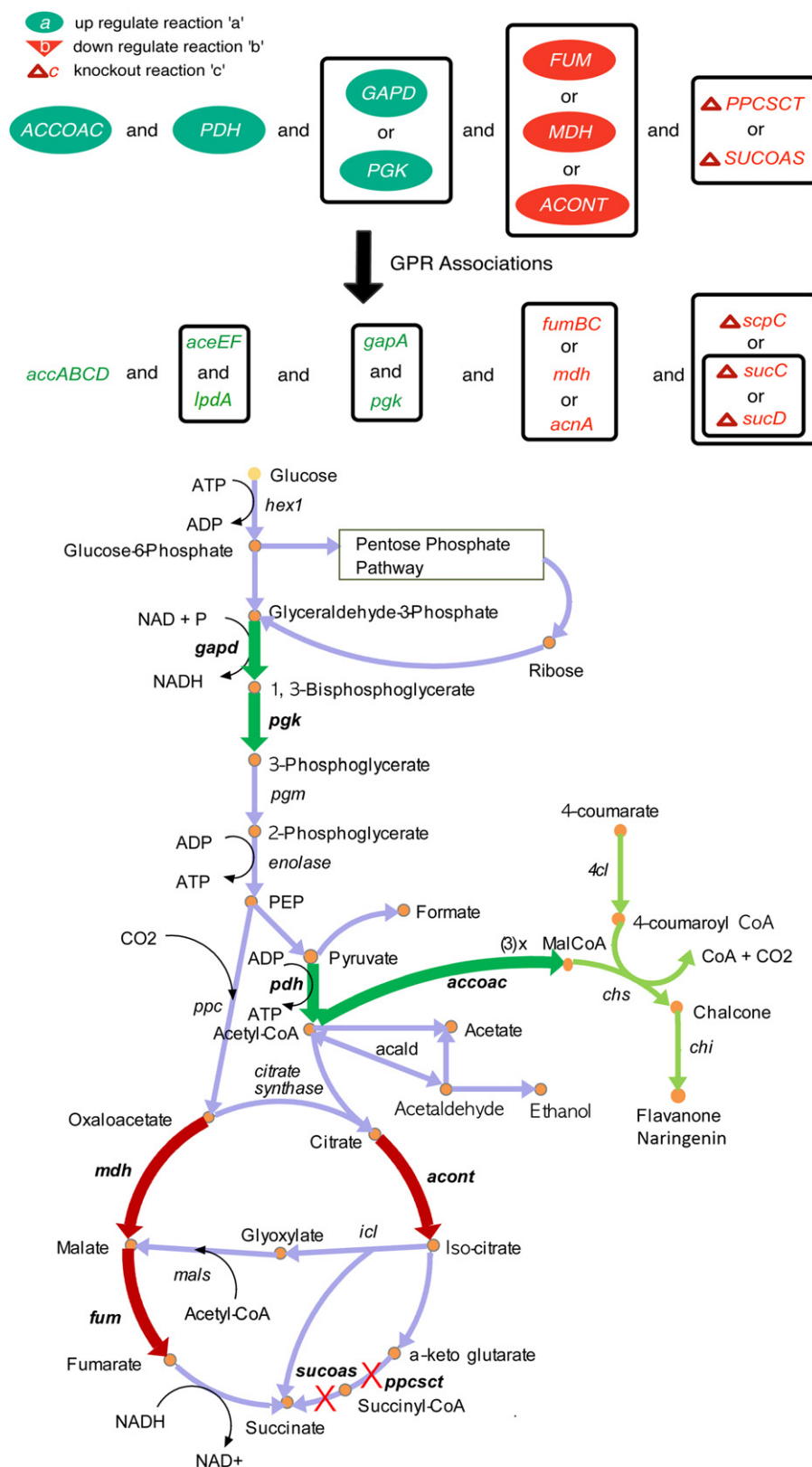


**Fig. 2.** Metabolic interventions predicted using OptForce procedure for overproducing naringenin in *E. coli*: In the metabolic map, reactions from the flavanone pathway are shown in light green and *E. coli* reactions are shown in light blue. Up-regulations are shown in dark green, down-regulations are shown in red and knockouts are indicated by  $\times$  symbol in red. ACCOAC: acetyl-CoA carboxylase encoded by *accABCD*; ACONT: aconitase encoded by *acnA* or *acnB*; FUM: fumarase encoded by *fumB* or *fumC*; GAPD: glyceraldehyde-3-phosphate dehydrogenase encoded by *gapA*; MDH: malate dehydrogenase encoded by *mdh*; PDH: pyruvate dehydrogenase complex encoded by *aceEF* and *lpdA*; PGK: phosphoglycerate kinase encoded by *pgk*; PPCSCT: propionyl-CoA succinate CoA transferase encoded by *scpC*; SUCOAS: succinyl-CoA synthetase encoded by *sucC* and *sucD*; 4CL: 4-coumaroyl-CoA ligase encoded by *4cl*; CHS: chalcone synthase encoded by *chs*; CHI: chalcone isomerase encoded by *chi*. (For interpretation of the references to color in this figure legend, the reader is referred to the web version of this article.)

Based on the above, it is important to note that the naringenin pathway requires the synthesis of two important precursors natively produced in *E. coli*—(1) acetyl-CoA that is produced at the end of glycolysis and pyruvate metabolism, and (2) malonyl-CoA, which is derived from the carboxylation of acetyl-CoA by acetyl-CoA carboxylase (ACCOAC). Acetyl-CoA serves as a key branching metabolite in redistributing resources to the citric acid cycle, fermentative byproducts and towards fatty acid and amino acid metabolism. On the other hand, malonyl-CoA participates in biomass formation directly as a reactant and through phospholipid biosynthesis and the synthesis of acyl carrier protein (ACP). However, the molar conversion ratio between glucose and malonyl-CoA is 1:1 under the assumption that half of the acetyl-CoA flux goes into TCA cycle. The requirements for malonyl-CoA are constrained by the allowances for cell growth, which in turn restricts the availability of malonyl-CoA for naringenin. Furthermore, the availability of malonyl-CoA imposes a restriction on the consumption of *p*-coumaric acid.

OptForce suggested the up-regulation of glycolytic reactions, namely glyceraldehyde-3-phosphate dehydrogenase (GAPD) and phosphoglycerate kinase (PGK) that would result in an increased flux towards pyruvate produced through glycolysis. In addition, up-regulation of pyruvate dehydrogenase (PDH) and acetyl-CoA carboxylase (ACCOAC) increase the pool of precursors acetyl-CoA and malonyl-CoA. In contrast, down-regulation of reactions in the citric acid cycle, namely malate dehydrogenase (MDH), fumarase (FUM) and aconitase (ACONTa/b), were suggested by OptForce to reduce the drain of carbon towards TCA cycle products. In order to allow for biomass production yield at 50% of the theoretical maximum, OptForce suggested reducing the activity of TCA reactions instead of completely eliminating them. Interestingly, OptForce predicted knockouts for the reactions succinyl-CoA synthetase (SUCCOAS) and propionyl-CoA:succinyl-CoA transferase (PPCSCT) that consume coenzyme A as a cofactor leading to the formation of succinyl-CoA. It is to be noted that the oxidation of pyruvate to acetyl-CoA by pyruvate dehydrogenase using coenzyme A is one of the key precursor reactions in the biosynthesis of malonyl-CoA. While the up-regulation of pyruvate dehydrogenase and acetyl-CoA carboxylase increase the utilization of coenzyme A towards the formation of malonyl-CoA, the remaining amount of coenzyme A is not sufficient for other parts of the metabolism. Notably, the wild-type flux values for reactions propionyl-CoA:succinyl-CoA transferase and succinyl-CoA synthetase indicate that a considerable amount of coenzyme A is utilized as a cofactor in the formation of succinyl-CoA and methylmalonyl-CoA. Hence, OptForce suggested completely eliminating these reactions in order to provide the maximum quantity of coenzyme A for the synthesis of malonyl-CoA.

### 3.2. Experimental procedures to implement OptForce predicted interventions

The interventions suggested by OptForce are at the metabolic flux level. In order to implement these interventions at the genetic level, it is essential to identify the genes encoding each one of these reactions. Using the gene-protein-reaction (GPR) associations provided with the iAF1260 metabolic model, we identified all genes (isozymes and subunits) encoding these reactions (Fig. 2). We selected the genes that were not regulated under our experimental conditions. For instance, *fumA*, *fumB* and *fumC* are three biochemically distinct fumarases (FUM) that catalyze the interconversion of fumarate to malate in the TCA cycle. Expression of these three isozymes in *E. coli* is controlled in a hierarchical manner depending on the environmental oxygen level (Tseng et al., 2001). Under our experimental conditions (see Section 2), RT-PCR profiling revealed that there is no detectable

*fumA* expression, which is consistent with the findings that *fumA* expression can only be activated under strict anaerobic conditions (Tseng et al., 2001). Similarly, the succinyl-coA synthetase of *E. coli* is encoded by two polycistronic genes, *sucC* ( $\beta$  subunit) and *sucD* ( $\alpha$  subunit), which are synthetic lethal pairs (Mottet et al., 2008; Suthers et al., 2009). After thoroughly scrutinizing the gene regulation under the experimental conditions and GPR associations, we selected the targets for genetic interventions for subsequent experiments.

### 3.3. Impact of TCA cycle disruptions on cell growth and flavanone biosynthesis

Acetyl-CoA is the first flux control point for polyphenol biosynthesis and is also an important metabolic intermediate connecting the central metabolic pathways involved in glycolysis, the TCA cycle and fatty acid biosynthesis. Under normal physiological conditions, the majority of acetyl-CoA flux will be driven into TCA cycle due to the relatively high affinity of citrate synthase ( $K_m=0.07$  mM) (Mothes et al., 1996). As such, down-regulation of TCA cycle can be regarded as a strategy to shunt the acetyl-CoA flux towards flavanone synthesis as proposed by the OptForce framework. While antisense RNA based gene silencing technology has been attempted for down-regulating post-transcriptional gene expression in recent years (Lee and Roth, 2003), achieving the anticipated down-regulation efficacy is difficult due to the lack of refined genetic circuits (gene expression control element) and the unstable nature of the RNA duplexes (i.e. terminal unpaired region, loop or hairpin degree) (Tummala et al., 2003). For this reason we decided to investigate only gene knockouts with no provisions for down-regulations.

Chromosomal inactivation of TCA cycle genes was carried out to identify flavanone-overproducing mutants with least effect on cell growth (Fig. 3). Results shown here indicate that single knockouts of *sucC*, *fumB* or *fumC* increased the production of naringenin, a common flavanone, by 30% compared to the wild type strain, whereas knockouts of *mdh*, *acnA* or *acnB* decreased naringenin production by up to 30–50% (note that OptForce suggested down-regulation **rather than** the knockouts for these TCA metabolic enzymes). However, specific naringenin production in the *mdh* and *acnA/B* mutant strains still outperformed the production achieved by the parental strain (23.9 mg/L/OD). It was also observed that naringenin production was positively coupled with cell density, demonstrating that the naringenin production objective was partially coincidental with the biomass objective, as

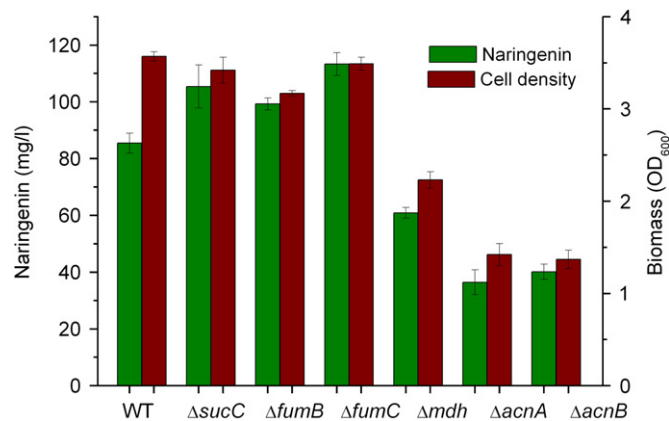


**Fig. 3.** Flavanone production and cell growth influenced by single gene knockout involved in tricarboxylic acid (TCA) cycle: Green bars represent naringenin production and red ones represent cell density. Error bars represent standard deviation of triplicate data points. (For interpretation of the references to color in this figure legend, the reader is referred to the web version of this article.)



and derive a better understanding of the underlying mechanisms that govern the flavanone recombinant pathway. As shown in Fig. 4, the two double mutants  $\Delta fumB\Delta sucC$  and  $\Delta fumC\Delta sucC$ , are promising combinations for the improvement of flavanone synthesis, while other double mutants including model-identified combinations (i.e.  $\Delta mdh\Delta sucC$ ) and intuitively inferred combinations (i.e.  $\Delta fumB\Delta fumC$ ) are less promising. Strains overexpressing acetyl-CoA carboxylase (ACC), phosphoglycerate kinase (PGK) and pyruvate dehydrogenase (PDH) in the  $\Delta fumC\Delta sucC$  double mutant background led to the maximum final volumetric production of 474 mg/L of naringenin, which is a 5.6-fold increase compared with the parental strain (85 mg/L). It was interesting to find that combinations of top single knockouts can result in suboptimal strains (i.e.  $\Delta fumB\Delta fumC$  double mutant strain) that yielded as low as 2/3 of the flavanone production level obtained from the best producer. Similarly, any additional modifications failed to further increase naringenin production compared with the *fumC* and *sucC* double mutant strain, probably due to the unbalanced metabolism between cell growth and product formation.

### 3.6. Enhanced cellular malonyl-CoA level in constructed strains

Cells tend to maintain a relatively constant level of acetyl-CoA and malonyl-CoA, something that severely limits their flavanone production potential (Fowler et al., 2009; Pitera et al., 2007). In order to verify our hypothesis that the constructed recombinant and mutant strains produced flavanones more efficiently due to higher levels of intracellular acetyl-CoA and malonyl-CoA, we measured the intracellular concentrations of these two cofactors in the engineered strains. Results shown here summarize the acetyl-CoA and malonyl-CoA levels in the engineered *E. coli* strain without expressing the flavanone pathway (Table 1) at different post-induction time points. Strains carrying acetyl-CoA carboxylase (ACC), phosphoglycerate kinase (PGK) and pyruvate dehydrogenase (PDH) overexpression in the *fumC* and *sucC* double mutant background were found to contain the highest levels of both malonyl-CoA and acetyl-CoA, which is consistent with the naringenin production profile (Fig. 4). Furthermore, the model-identified optimal strains (*fumC* and *sucC* double mutants) exhibit a relatively high level of acetyl-CoA ( $\sim 11.6 \mu\text{mol/gDW}$ ) and malonyl-CoA ( $\sim 10.4 \mu\text{mol/gDW}$ ), roughly a 4-fold increase over the wild type strain, indicating that the TCA cycle was severely impaired and the carbon flux was successfully rerouted to the acetyl-CoA and malonyl-CoA synthesis compared with the single knockout or wild type strain. Moreover, for the suboptimal strains ( $\Delta acnB$  and  $\Delta mdh\Delta sucC$  mutants), the changing pattern of malonyl-CoA levels at different post-induction phase resembled the ones from the wild type strain, indicating that other possible limiting factors, such as lack of precursor availability, unbalanced  $\text{NAD}^+/\text{NADH}$  ratio or impaired glyoxylate shunt pathway, may cancel the beneficial effects of these genetic interventions. As mentioned before,

reduced cell growth associated with these interventions is a genuine factor that may affect the malonyl-CoA level.

Malonyl-CoA availability has been shown to be a rate-limiting factor for an array of ATP dependent chain initiation and elongation reactions involved in fatty acid, flavonoid and polyketide biosynthesis (Liu et al., 2010; Xu and Koffas, 2010; Zha et al., 2009). As such, significant metabolic engineering efforts have been dedicated to cellular malonyl-CoA improvement. It should be noted that the downstream malonyl-CoA competing pathway, malonyl-CoA:ACP transacetylase (encoded by *fabD*) which catalyzes the committed step for fatty acids synthesis, was excluded as a knock-out target because knockout of *fabD* results in a nonviable phenotype (Handke et al., 2011).

## 4. Discussion

### 4.1. Validating computational predictions from OptForce

In this work, we have successfully validated computational predictions from OptForce (Ranganathan and Maranas, 2010; Ranganathan et al., 2010) by designing a strain of *E. coli* with increased levels of intracellular malonyl-CoA. In essence, by implementing a minimal number of direct metabolic interventions (i.e. FORCE sets), we were able to alter the wild-type metabolic network of the microbe towards meeting the changes (encoded within the MUST sets) that conform to our overproduction objective. The set of alternative interventions predicted by OptForce enabled us to avoid genetic interventions that are more difficult to perform or less viable under the experimental conditions. By exhaustively exploring all alternative optimal solutions, FORCE sets can be represented in the form of decision-tree where some interventions can be substituted with others. For example, as shown in Fig. 2, the knockouts for propionyl-CoA:succinyl-CoA transferase can be substituted by the deletion of succinyl-CoA synthetase. Additionally, interventions predicted by OptForce are rank-ordered based on their quantitative impact towards satisfying the overproduction target. For example, when only three modifications were allowed, OptForce chose the upregulation of acetyl-CoA carboxylase, pyruvate dehydrogenase and glycolytic reactions that collectively resulted in a yield of 33% of the target yield. As shown in Fig. 5, the absolute yields for naringenin increase by about 200% from the wild-type by just including up-regulations for the genes *accA* and *gapA* or *pgk*. For five interventions ( $k=5$ ), the original upregulations were conserved and in addition OptForce predicted knockouts for succinyl-CoA synthetase and down regulations in the TCA cycle that enabled meeting the imposed target. Knockouts for genes *mdh* and *acnA* severely compromised the formation of biomass and naringenin. Note that OptForce suggested down-regulating as opposed to completely eliminating the activity of these reactions. However,

**Table 1**

Intracellular malonyl-CoA and acetyl-CoA ( $\mu\text{mol/gDW}$ ) accumulated in engineered *E. coli* strain without the expression of flavanone pathway at different post-induction phase (0, 3 and 15 h).

Genotype	Malonyl-CoA ( $\mu\text{mol/gDW}$ )			Acetyl-CoA ( $\mu\text{mol/gDW}$ )		
	0 h	3 h	15 h	0 h	3 h	15 h
WT	2.71 $\pm$ 0.41	2.80 $\pm$ 0.39	2.55 $\pm$ 0.46	2.15 $\pm$ 0.09	2.54 $\pm$ 0.48	3.83 $\pm$ 0.34
WT with ACC, PGK	3.66 $\pm$ 0.40	3.89 $\pm$ 0.31	3.84 $\pm$ 0.46	3.53 $\pm$ 0.71	3.71 $\pm$ 0.45	4.91 $\pm$ 0.74
$\Delta sucC$ with ACC, PGK	3.83 $\pm$ 0.34	4.29 $\pm$ 0.60	5.76 $\pm$ 1.04	4.28 $\pm$ 0.17	4.85 $\pm$ 0.39	5.23 $\pm$ 0.84
$\Delta fumC$ with ACC, PGK	3.57 $\pm$ 0.61	5.36 $\pm$ 0.27	6.84 $\pm$ 1.23	4.43 $\pm$ 0.18	5.09 $\pm$ 0.61	5.41 $\pm$ 0.92
$\Delta acnB$ with ACC, PGK	2.84 $\pm$ 0.26	2.90 $\pm$ 0.52	2.87 $\pm$ 0.29	2.38 $\pm$ 0.24	3.53 $\pm$ 0.39	4.07 $\pm$ 0.69
$\Delta mdh\Delta sucC$ with ACC, PGK	3.86 $\pm$ 0.19	4.89 $\pm$ 0.59	4.98 $\pm$ 0.80	4.15 $\pm$ 0.37	5.47 $\pm$ 0.66	5.83 $\pm$ 0.52
$\Delta fumC\Delta sucC$	3.02 $\pm$ 0.18	4.93 $\pm$ 0.79	5.87 $\pm$ 0.65	5.04 $\pm$ 0.55	6.12 $\pm$ 0.98	8.46 $\pm$ 0.59
$\Delta fumC\Delta sucC$ with ACC, PGK, PDH	3.96 $\pm$ 0.59	6.17 $\pm$ 0.56	10.35 $\pm$ 0.72	5.74 $\pm$ 0.86	6.69 $\pm$ 0.47	11.63 $\pm$ 1.16

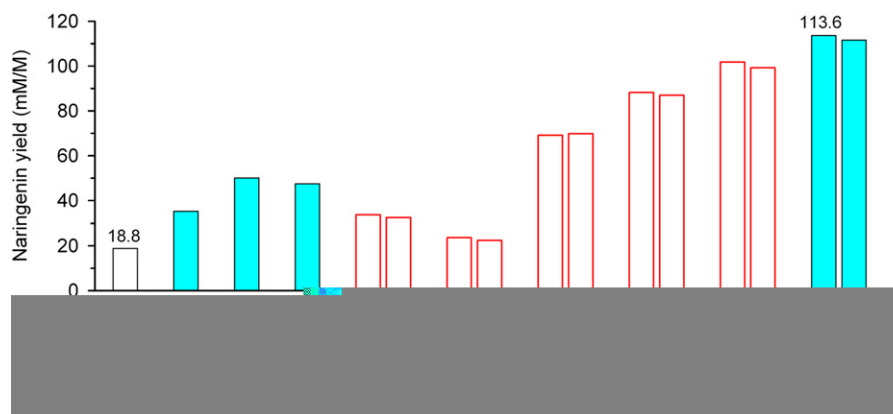


**Fig. 5.** Plot between naringenin yield and the number of genetic interventions ( $k$ ) that were predicted by OptForce procedure. Overexpressions are shown in green and knockouts are shown in red. (For interpretation of the references to color in this figure legend, the reader is referred to the web version of this article.)

as we stated earlier, we exclusively implemented knockouts whenever OptForce suggested either reaction eliminations or down-regulations. In addition, products of these reactions are closely associated with the formation of biomass. For this reason, we decided to investigate alternative gene knockouts (i.e. *fumB* and *fumC*) proposed by OptForce. Furthermore, knockouts for *fumC* and *sucC* in combination with overexpression of three subunits enzyme pyruvate dehydrogenase further boosted the yield of naringenin to 113.6 mM/M of glucose (Fig. 5).

#### 4.2. Synergistic effect of gene knockout and overexpression on the yields

Impact of independent genetic interventions on cellular phenotype can be additive due to the interactions among the interconnected pathways. Here we introduce a simple analysis method that would allow the assessment of gene interactions and their impact on a specific cellular phenotype on the pathway level. First, naringenin yield coefficient from glucose was experimentally determined from the steady state naringenin formation rate and glucose consumption rate (Supplemental Figure S3 ABC). A relative yield change when comparing the parental wild type strain to the strains harboring overexpression or knockout modifications can be calculated according to the proposed equation in the supplemental files (Supplemental Equation 1). Then a synergistic coefficient  $\varphi$  can be extracted for evaluating to which extent the investigated genes coupled together to affect a prescribed phenotype. Generally, the impact of multiple genetic interventions on production can follow two patterns: additive effects ( $\varphi=0$ ) which essentially reflect two entirely unrelated pathways; and synergistic effects ( $\varphi \neq 0$ ) which reflect two closely related or interconnected pathways (such as the native glycolysis and TCA pathway).

It was found that the impact of multiple genetic interventions identified by OptForce on naringenin yield change is more complex than the simple additive contribution of the single genetic interventions (Fig. 6). For example, combinations of positive genetic interventions result in a yield change much higher than the sum of the individual contributions ( $\varphi > 0$ ); on the contrary, combinations of positive and negative genetic interventions lead to a yield change much lower than the sum of the individual contributions ( $\varphi < 0$ ). This observation clearly indicates that there is no additive effect but rather a synergistic effect (positive or negative cooperativity) among the model-predicted modifications. The negative coefficient indicates one or several of the investigated genes negatively dominate the prescribed phenotype, which should be excluded for combinatorial consideration (i.e. the *mdh* and *acnB* mutant strain in Fig. 6).

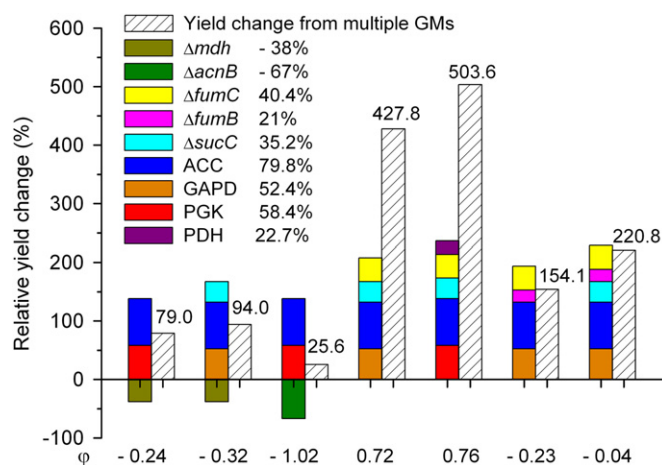


**Fig. 6.** Mapping the synergistic effects of gene knockout and overexpression on the relative yield change of naringenin from glucose: Color-coded stacking columns represent the cumulative yield change resulting from single gene overexpression or knockout; the relative yield change corresponding to each genetic modification has been indicated by the specific number following each colored label (For example, overexpression of ACC can lead to a 79.8% increase). Each color bar represents a single genetic intervention. The sparse bar represents the total yield change resulting from combinations of genetic interventions compared to wild type strain, as specified by the value on top of the corresponding column. Synergistic coefficient  $\varphi$  for each of the intervention combinations are also indicated underneath the corresponding column in this figure. (For interpretation of the references to color in this figure legend, the reader is referred to the web version of this article.)

The larger of this coefficient, the stronger synergistic effect can be found in the investigated gene clusters on the production phenotype, which can serve as a guideline for selecting combinatorial genetic interventions for strain optimization. However, this conclusion apparently does not apply to the intuitively inferred strains (i.e.  $\Delta fumB\Delta fumC$  double mutant, Fig. 6), which were constructed by stacking together the top single knockouts predicted by OptForce (as will be discussed later). Quantitative description of multiple genetic interventions on cell phenotype is therefore important for investigating genotype-phenotype interactions motivating the use of computational tools such as OptForce for strain optimization.

#### 4.3. Exploration of flavanone phenotype phase plane under combinatorial gene knockout and overexpression constraints

Phenotype phase planes (Fig. 7) constructed by linking the closely-related kinetic information with a specific phenotype

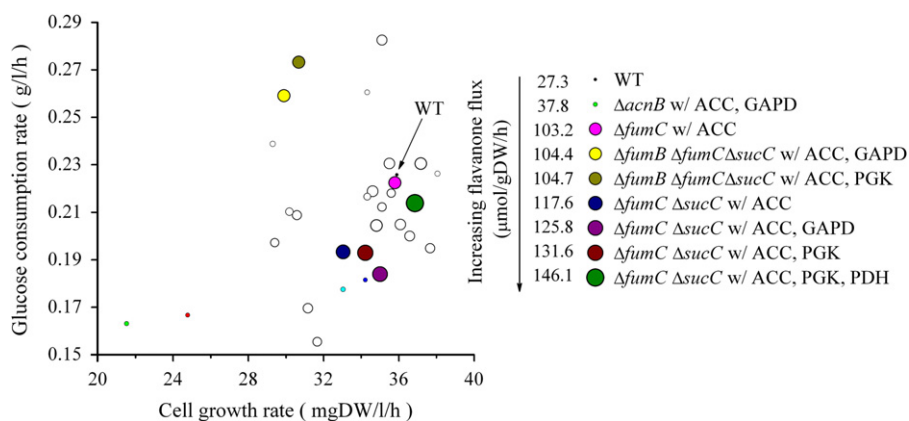


**Fig. 7.** Characterization of the flavanone flux distribution resulting from combinatorial gene knockout and overexpression in the phenotype phase plane. Flavanone flux ( $\mu\text{mol/gDW/h}$ ) was determined based on steady state flavanone production rate and cell density increase in 36-h shake-flask fermentation. The circular area represents the relative naringenin flux distribution of the engineered *E. coli* strain. Part of the representative strain genotypes has been color-labeled. (For interpretation of the references to color in this figure legend, the reader is referred to the web version of this article.)

(such as flavanone flux distribution), can be used for more quantitative investigation of cell metabolism and identification of unknown issues associated with genetic interventions (Blazek and Alper, 2010). As shown in Fig. 7, the *fumC* and *sucC* double mutant strain carrying overexpressions of ACC, PGK and PDH, resulted in a flux through the flavanone recombinant pathway of  $146.1 \mu\text{mol/gDW/h}$ , a 5.4 times increase compared to the wild type strain ( $27.3 \mu\text{mol/gDW/h}$ ). In addition, most of the optimal and suboptimal candidate strains share similar phenotypes such as higher cell growth rate and moderate glucose consumption rate compared with the wild type strain, which might be crucial for balancing growth requirements on one hand and heterologous pathway expression on the other. However, the triple knockout strain  $\Delta\textit{fumB}\Delta\textit{fumC}\Delta\textit{sucC}$  exhibits a much higher glucose consumption rate but lower cell growth rate, indicating that cellular metabolism is severely impaired as a result of either a futile TCA cycle or toxic compound accumulation due to the complete disruption of TCA cycle, as evidenced that a significantly higher level of acetate (more than 30 mM) has been detected in this triple knockout strain.

## 5. Conclusions

In this study, we have described an integrated computational and experimental approach for enhancing carbon flux towards malonyl-CoA in *E. coli*, a key precursor in natural product biosynthesis such as flavonoids and polyketides. Unlike previous work on this topic, the metabolic engineering strategy developed and applied in this manuscript is based on the real metabolic flux data that largely pinpoint the physiological state of the host strain. This genome-scale computational approach to metabolic networks takes into consideration the complex interconnectivity of cellular metabolism and allows the prediction of minimal set of genetic interventions that guarantee a prescribed phenotype, which are not obvious to predict by network inspection. Even more, it allows the identification of optimal combinations of gene knockouts and overexpressions which can prioritize the implementation of genetic interventions. We have successfully identified the interventions that cooperatively force carbon flux towards malonyl-CoA and demonstrated the sequential aggregation of beneficial interventions, which in turn resulted in a 560% increase in the volumetric flavanone production ( $474 \text{ mg/L}$ ) from a recombinant *E. coli* strain. Genetic interventions for improving cellular malonyl-CoA and acetyl-CoA level highlight the potential not only for flavonoid biosynthesis but other commercially-important compounds like fatty acids, polyketides and biodiesels.

## Competing interests

The authors declare that they have no conflict of interest.

## Acknowledgments

We acknowledge the financial support from the Independent Research and Development Fund awarded to M.A.G. Koffas from the State University of New York at Buffalo.

## Appendix A. Supplementary materials

Supplementary data associated with this article can be found in the online version at doi:10.1016/j.ymben.2011.06.008.

## References

- Alper, H., Jin, Y.-S., Moxley, J.F., Stephanopoulos, G., 2005. Identifying gene targets for the metabolic engineering of lycopene biosynthesis in *Escherichia coli*. *Metab. Eng.* 7, 155–164.
- Askenazi, M., Driggers, E.M., Holtzman, D.A., Norman, T.C., Iverson, S., Zimmer, D.P., Boers, M.E., Blomquist, P.R., Martinez, E.J., Monreal, A.W., Feibelman, T.P., Mayorga, M.E., Maxon, M.E., Sykes, K., Tobin, J.V., Cordero, E., Salama, S.R., Trueheart, J., Royer, J.C., Madden, K.T., 2003. Integrating transcriptional and metabolite profiles to direct the engineering of lovastatin-producing fungal strains. *Nat. Biotechnol.* 21, 150–156.
- Blazek, J., Alper, H., 2010. Systems metabolic engineering: genome-scale models and beyond. *Biotechnol. J.* 5, 647–659.
- Burgard, A.P., Maranas, C.D., 2001. Probing the performance limits of the *Escherichia coli* metabolic network subject to gene additions or deletions. *Biotechnol. Bioeng.* 74, 364–375.
- Burgard, A.P., Pharkya, P., Maranas, C.D., 2003. Optknock: a bilevel programming framework for identifying gene knockout strategies for microbial strain optimization. *Biotechnol. Bioeng.* 84, 647–657.
- Cahoon, E.B., Shockey, J.M., Dietrich, C.R., Gidda, S.K., Mullen, R.T., Dyer, J.M., 2007. Engineering oilseeds for sustainable production of industrial and nutritional feedstocks: solving bottlenecks in fatty acid flux. *Curr. Opin. Plant. Biol.* 10, 236–244.
- Chemler, J.A., Koffas, M.A., 2008. Metabolic engineering for plant natural product biosynthesis in microbes. *Curr. Opin. Biotechnol.* 19, 597–605.
- Cragg, G.M., Newman, D.J., Snader, K.M., 1997. Natural products in drug discovery and development. *J. Nat. Prod.* 60, 52–60.
- Datsenko, K.A., Wanner, B.L., 2000. One-step inactivation of chromosomal genes in *Escherichia coli* K-12 using PCR products. *Proc. Natl. Acad. Sci. USA* 97, 6640–6645.
- Davis, M.S., Solbiati, J., Cronan Jr., J.E., 2000. Overproduction of acetyl-CoA carboxylase activity increases the rate of fatty acid biosynthesis in *Escherichia coli*. *J. Biol. Chem.* 275, 28593–28598.
- Dobson, P., Smallbone, K., Jameson, D., Simeonidis, E., Lanthaler, K., Pir, P., Lu, C., Swainston, N., Dunn, W., Fisher, P., Hull, D., Brown, M., Oshota, O., Stanford, N.,

- Kell, Y., King, R., Oliver, S., Stevens, R., Mendes, P., 2010. Further developments towards a genome-scale metabolic model of yeast. *BMC Systems Biol.* 4, 145.
- Feist, A.M., Henry, C.S., Reed, J.L., Krummenacker, M., Joyce, A.R., Karp, P.D., Broadbelt, L.J., Hatzimanikatis, V., Palsson, B.O., 2007. A genome-scale metabolic reconstruction for *Escherichia coli* K-12 MG1655 that accounts for 1260 ORFs and thermodynamic information. *Mol. Syst. Biol.* 3, 121.
- Feist, A.M., Palsson, B.O., 2008. The growing scope of applications of genome-scale metabolic reconstructions using *Escherichia coli*. *Nat. Biotechnol.* 26, 659–667.
- Fischer, E., Zamboni, N., Sauer, U., 2004. High-throughput metabolic flux analysis based on gas chromatography-mass spectrometry derived  $^{13}\text{C}$  constraints. *Anal. Biochem.* 325, 308–316.
- Fowler, Z.L., Gikandi, W.W., Koffas, M.A., 2009. Increasing Malonyl-CoA biosynthesis by tuning the *Escherichia coli* metabolic network and its application to flavanone production. *Appl. Environ. Microbiol.* 75, 5831–5839.
- Handke, P., Lynch, S.A., Gill, R.T., 2011. Application and engineering of fatty acid biosynthesis in *Escherichia coli* for advanced fuels and chemicals. *Metab. Eng.* 13, 28–37.
- Harborne, J.B., Williams, C.A., 1975. *The Flavonoids*. Chapman and Hall, London, United Kingdom, pp. 127–313.
- Kalscheuer, R., Stolting, T., Steinbuechel, A., 2006. Microdiesel: *Escherichia coli* engineered for fuel production. *Microbiology* 152, 2529–2536.
- Khosla, C., Keasling, J.D., 2003. Metabolic engineering for drug discovery and development. *Nat. Rev. Drug. Discov.* 2, 1019–1025.
- Kim, J., Reed, J.L., 2010. OptORF: Optimal metabolic and regulatory perturbations for metabolic engineering of microbial strains. *BMC Syst. Biol.* 4, 53.
- Lee, L.K., Roth, C.M., 2003. Antisense technology in molecular and cellular bioengineering. *Curr. Opin. Biotechnol.* 14, 505–511.
- Leonard, E., Lim, K.-H., Saw, P.-N., Koffas, M.A.G., 2007. Engineering central metabolic pathways for high-level flavonoid production in *Escherichia coli*. *Appl. Environ. Microbiol.* 73, 3877–3886.
- Leonard, E., Yan, Y., Fowler, Z.L., Li, Z., Lim, C.G., Lim, K.H., Koffas, M.A., 2008. Strain improvement of recombinant *Escherichia coli* for efficient production of plant flavonoids. *Mol. Pharm.* 5, 257–265.
- Lim, C., Fowler, Z., Hueller, T., Schaffer, S., Koffas, M., 2011. High-yield resveratrol production in engineered *Escherichia coli*. *Appl. Environ. Microbiol.* 77, 3451–3460.
- Liu, T., Vora, H., Khosla, C., 2010. Quantitative analysis and engineering of fatty acid biosynthesis in *E. coli*. *Metab. Eng.* 12, 378–386.
- Magnuson, K., Jackowski, S., Rock, C.O., Cronan Jr., J.E., 1993. Regulation of fatty acid biosynthesis in *Escherichia coli*. *Microbiol. Rev.* 57, 522–542.
- Mahadevan, R., Schilling, C.H., 2003. The effects of alternate optimal solutions in constraint-based genome-scale metabolic models. *Metab. Eng.* 5, 264–276.
- Mothes, G., Rivera, I.S., Babel, W., 1996. Competition between beta-ketothiolase and citrate synthase during poly(beta-hydroxybutyrate) synthesis in *Methylobacterium rhodesianum*. *Arch. Microbiol.* 166, 405–410.
- Motter, A.E., Gulbahce, N., Almaas, E., Barabasi, A.L., 2008. Predicting synthetic rescues in metabolic networks. *Mol. Syst. Biol.* 4, 168.
- Noronha, S.B., Yeh, H.J., Spande, T.F., Shiloach, J., 2000. Investigation of the TCA cycle and the glyoxylate shunt in *Escherichia coli* BL21 and JM109 using (13)C-NMR/MS. *Biotechnol. Bioeng.* 68, 316–327.
- Park, J.H., Lee, K.H., Kim, T.Y., Lee, S.Y., 2007. Metabolic engineering of *Escherichia coli* for the production of L-valine based on transcriptome analysis and in silico gene knockout simulation. *Proc. Natl. Acad. Sci. USA* 104, 7797–7802.
- Pfeifer, B.A., Khosla, C., 2001. Biosynthesis of polyketides in heterologous hosts. *Microbiol. Mol. Biol. Rev.* 65, 106–118.
- Pharkya, P., Burgard, A.P., Maranas, C.D., 2003. Exploring the overproduction of amino acids using the bilevel optimization framework OptKnock. *Biotechnol. Bioeng.* 84, 887–899.
- Pharkya, P., Maranas, C.D., 2006. An optimization framework for identifying reaction activation/inhibition or elimination candidates for overproduction in microbial systems. *Metab. Eng.* 8, 1–13.
- Pitera, D.J., Paddon, C.J., Newman, J.D., Keasling, J.D., 2007. Balancing a heterologous mevalonate pathway for improved isoprenoid production in *Escherichia coli*. *Metab. Eng.* 9, 193–207.
- Qi, B.X., Fraser, T., Mugford, S., Dobson, G., Sayanova, O., Butler, J., Napier, J.A., Stobart, A.K., Lazarus, C.M., 2004. Production of very long chain polyunsaturated omega-3 and omega-6 fatty acids in plants. *Nat. Biotechnol.* 22, 739–745.
- Ranganathan, S., Maranas, C.D., 2010. Microbial 1-butanol production: identification of non-native production routes and in silico engineering interventions. *Biotechnol. J.* 5, 716–725.
- Ranganathan, S., Suthers, P.F., Maranas, C.D., 2010. OptForce: an optimization procedure for identifying all genetic manipulations leading to targeted overproductions. *PLoS Comput. Biol.* 6, e1000744.
- Sauer, U., 2006. Metabolic networks in motion:  $^{13}\text{C}$ -based flux analysis. *Mol. Syst. Biol.* 2, 62.
- Schaub, J., Mauch, K., Reuss, M., 2008. Metabolic flux analysis in *Escherichia coli* by integrating isotopic dynamic and isotopic stationary  $^{13}\text{C}$  labeling data. *Biotechnol. Bioeng.* 99, 1170–1185.
- Schwender, J., 2008. Metabolic flux analysis as a tool in metabolic engineering of plants. *Curr. Opin. Biotechnol.* 19, 131–137.
- Segre, D., Vitkup, D., Church, G.M., 2002. Analysis of optimality in natural and perturbed metabolic networks. *Proc. Natl. Acad. Sci. USA* 99, 15112–15117.
- Suthers, P.F., Zomorodi, A., Maranas, C.D., 2009. Genome-scale gene/reaction essentiality and synthetic lethality analysis. *Mol. Syst. Biol.* 5, 301.
- Takamura, Y., Nomura, G., 1988. Changes in the intracellular concentration of acetyl-CoA and malonyl-CoA in relation to the carbon and energy metabolism of *Escherichia coli* K12. *J. Gen. Microbiol.* 134, 2249–2253.
- Tepper, N., Shlomi, T., 2009. Predicting metabolic engineering knockout strategies for chemical production: accounting for competing pathways. *Bioinformatics* 26, 536–543.
- Tseng, C.P., Yu, C.C., Lin, H.H., Chang, C.Y., Kuo, J.T., 2001. Oxygen- and growth rate-dependent regulation of *Escherichia coli* fumarase (FumA, FumB, and FumC) activity. *J. Bacteriol.* 183, 461–467.
- Tummala, S.B., Welker, N.E., Papoutsakis, E.T., 2003. Design of antisense RNA constructs for downregulation of the acetone formation pathway of *Clostridium acetobutylicum*. *J. Bacteriol.* 185, 1923–1934.
- van de Walle, M., Shiloach, J., 1998. Proposed mechanism of acetate accumulation in two recombinant *Escherichia coli* strains during high density fermentation. *Biotechnol. Bioeng.* 57, 71–78.
- Wattanachaisaareekul, S., Lantz, A.E., Nielsen, M.L., Nielsen, J., 2008. Production of the polyketide 6-MSA in yeast engineered for increased malonyl-CoA supply. *Metab. Eng.* 10, 246–254.
- Winkel-Shirley, B., 2001. Flavonoid biosynthesis. a colorful model for genetics, biochemistry, cell biology, and biotechnology. *Plant Physiol.* 126, 485–493.
- Xu, P., Koffas, M.A.G., 2010. Metabolic engineering of *Escherichia coli* for biofuel production. *Biofuels* 1, 493–504.
- Yan, Y., Kohli, A., Koffas, M.A., 2005. Biosynthesis of natural flavanones in *Saccharomyces cerevisiae*. *Appl. Environ. Microbiol.* 71, 5610–5613.
- Zha, W., Rubin-Pitel, S.B., Shao, Z., Zhao, H., 2009. Improving cellular malonyl-CoA level in *Escherichia coli* via metabolic engineering. *Metab. Eng.* 11, 192–198.
- Zhang, W., Li, Y., Tang, Y., 2008. Engineered biosynthesis of bacterial aromatic polyketides in *Escherichia coli*. *Proc. Natl. Acad. Sci. USA* 105, 20683–20688.
- Zomorodi, A.R., Maranas, C.D., 2010. Improving the iMM904 *S. cerevisiae* metabolic model using essentiality and synthetic lethality data. *BMC. Syst. Biol.* 4, 178.